

# Dispersion of Discontinuous Periodic Waves

Gong Chen  
School of Mathematics  
University of Minnesota  
Minneapolis, MN 55455  
chenx563@umn.edu

Peter J. Olver<sup>†</sup>  
School of Mathematics  
University of Minnesota  
Minneapolis, MN 55455  
olver@umn.edu  
<http://www.math.umn.edu/~olver>

**Abstract.** The dynamic evolution of linearly dispersive waves on periodic domains with discontinuous initial profiles is shown to depend dramatically upon the asymptotics of the dispersion relation at large wave number. Asymptotically linear or sublinear dispersion relations produce slowly changing waves, while those with polynomial growth exhibit dispersive quantization, a.k.a. the Talbot effect, being (approximately) quantized at rational times, but a non-differentiable fractal at irrational times. Numerical experiments suggest that such effects persist into the nonlinear regime, for both integrable and non-integrable systems. Implications for the successful modeling of wave phenomena on bounded domains and numerical challenges are discussed.

---

<sup>†</sup> *Supported in part by NSF Grant DMS 11-08894.*

November 12, 2012

## 1. Introduction.

The most common device used to model physical wave phenomena is to approximate the fully nonlinear fluid mechanics problem in a targeted physical regime by first suitably rescaling the original variables and then expanding the rescaled system in powers of an appropriate small parameter. Truncation at low (typically first) order produces a mathematically simpler system, whose solutions, one hopes, closely track the originals, at least over an initial time span.

At the linear level (at least in the homogeneous, isotropic regime), conservative wave dynamics is entirely determined by the dispersion relation, which relates the temporal frequency of an oscillatory complex exponential solution to its wave number (spatial frequency). The standard modeling paradigm can thus, at the linear level, be viewed as replacing the full dispersion relation by a suitable approximation. However, in most perturbative models, while the approximate dispersion relation is designed to fit its physical counterpart well at small wave numbers, e.g., they have the same Taylor polynomial at the origin, they often have little in common at the high frequency range. For example, the free boundary problem governing water waves has a dispersion relation that is asymptotically proportional to a square root of the wave number. On the other hand, in the shallow water regime, the unidirectional Korteweg–deVries model’s dispersion relation is cubic, and of the wrong sign, the competing Regularized Long Wave (RLW) or Benjamin–Bona–Mahony (BBM) model’s is asymptotically zero, while that of some standard bidirectional Boussinesq systems is asymptotically constant. Provided one restricts attention to smooth solutions, or to unbounded domains, the discrepancies in the dispersion of high frequency modes do not seem to play a very noticeable role. However, on bounded domains, rougher solutions, which have more substantial high frequency components, are affected in a significant manner owing to subtle and as yet poorly understood resonances among the varyingly propagating Fourier modes.

In, [38], the second author observed that, for integral polynomial dispersion relations, i.e., those whose coefficients are integer multiples of a common real number  $\lambda$ , the solution in question has the remarkable behavior that, at irrational times (relative to the ratio  $\beta = \ell/\lambda$  between the length  $\ell$  of the interval and the dispersion constant  $\lambda$ ), it is a continuous, but fractal, non-differentiable function, whereas at rational times, the solution is piecewise constant! While previously unnoticed<sup>†</sup> by experts in dispersive wave theory, the phenomenon of dispersive quantization had, in fact, been first discovered in the early 1990’s, in the contexts of optics and quantum mechanics, by Michael Berry and various collaborators, [2, 3, 4, 6, 23], who named it the *Talbot effect* in honor of a striking 1836 optical experiment by the photographic pioneer William Henry Fox Talbot, [46]. Experimental confirmations of the Talbot effect in optics and in quantum revival are described in [6]. Rigorous analytical results and estimates justifying the Talbot effect can be found in the work of Kapitanski and Rodnianski, [27, 43], Oskolkov, [40, 41], and Taylor, [47].

---

<sup>†</sup> The work of Oskolkov, [41], which analyzes both the linear Schrödinger equation and the linearized Korteweg–deVries equation on periodic domains, is a notable exception.

The initial aim of the present paper is to extend these studies to basic linear differential and integro-differential equations, depending on a single spatial variable, that have non-polynomial dispersion relations. Our main conclusion is that the large wave number asymptotics of the dispersion relation plays the dominant role governing the qualitative features exhibited by their rough solutions on periodic domains. In analogy with the basic Riemann problem of gas dynamics, [53], we focus on the specific initial data provided by a step function. The resulting Fourier series solution is easily constructed, and of independent interest. For example, when the dispersion relation is polynomial, the solution at rational times has the form of a Gauss or Weyl exponential sum, of fundamental importance in analytic number theory since the work of Hardy, Littlewood, and Vinogradov, [24, 51]. Indeed, as explained in [22], since the behavior of such exponential sums has implications for the size of the zero-free region of the Riemann zeta function in the critical strip, further refinement of known estimates could provide a route to proving the Riemann hypothesis!

We will also initiate the investigation of such effects in the nonlinear regime. The revolutionary discovery of the *soliton* was sparked by the original movie of Zabusky and Kruskal, [55], that displayed a numerical simulation of the solution to a particular periodic initial-boundary value problem for the Korteweg–deVries equation with small nonlinearity. (In contrast, the celebrated studies of Lax, Levermore, and Venakides, [31, 32, 49, 50], are concerned with the small dispersion regime and convergence to shock wave solutions of the limiting nonlinear transport equation.) Because Zabusky and Kruskal’s selected initial data was a smoothly varying cosine, the Talbot fractalization effect was (perhaps fortunately!) not observed. (And, technically, the elastically interacting waves that emerge from the initial cosine profile are not true solitons, in that these only exist for the full line problem, but, rather, cnoidal waves embedded in a hyperelliptic finite gap solution, [30, 34].) Our numerical experiments with step function initial data strongly indicate that the dispersive quantization/fractalization effect is present in the periodic boundary value problems for both the integrable nonlinear Korteweg–deVries and Schrödinger equations, as well as non-integrable models of a similar nature, and extends well beyond the weakly nonlinear regime.

One consequence of these studies is that, contrary to the conventional wisdom, when dealing with nonlinear wave models on bounded intervals, the principal source of analytic difficulty may be, counterintuitively, not the nonlinear terms, but rather the poorly understood behavior of linearly dispersive partial differential equations. Our investigations imply that the qualitative behavior of the solution to the periodic problem depends crucially on the asymptotic behavior of the dispersion relation at large wave number, reinforcing Benjamin et. al.’s critique, [1], that the Korteweg–deVries equation, say, is an unsatisfactory model for surface waves because its cubic dispersion relation effectively transmits the high frequency modes in the wrong direction, with unboundedly negative phase velocity and group velocity, inciting unphysical interactions with other solution components. And indeed, in the periodic problem, this shortcoming is observed as the apparently number-theoretic resonant interaction of high frequency modes spawned by the initial data serve to produce a-physical fractalization and quantization effects in the engendered solution.

## 2. Dispersion Relations and Wave Models.

Consider a linear, scalar, constant coefficient partial differential equation for a function  $u(t, x)$  of time  $t$  and a single spatial variable  $x$ . Recall, [53], that the *dispersion relation*  $\omega(k)$  relates temporal frequency  $\omega$  to wave number (spatial frequency)  $k$  of an oscillatory complex exponential solution of the form

$$u(t, x) = e^{i(kx - \omega t)}. \quad (2.1)$$

The differential equation will be called *purely dispersive* if the resulting function  $\omega(k)$  is real. (Complex dispersion relations indicate the presence of dissipative or viscous effects that damp out solutions, or, alternatively, ill-posedness, depending on the sign of their imaginary part.) Given a real dispersion relation, the *phase velocity*  $c_p = \omega(k)/k$  prescribes the speed of an individual oscillatory wave, while, as a consequence of the method of stationary phase, wave packets and energy move with the *group velocity*  $c_g = d\omega/dk$ , [53]. These differ when the dispersion relation is nonlinear, causing initially localized disturbances to spread out in a dispersive fashion — a physical effect that can be seen, for example, by throwing a rock into a pond and observing that the individual waves move at a different speed, namely the phase velocity, than the overall disturbance, which moves at the group velocity. The dispersion relation of nonlinear equations is that of their linearization.

For example, the basic *transport equation*

$$u_t + c u_x = 0 \quad (2.2)$$

has linear dispersion relation  $\omega(k) = ck$ , while the one-dimensional *wave equation*

$$u_{tt} = c^2 u_{xx} \quad (2.3)$$

has bidirectional dispersion relation  $\omega(k) = \pm ck$ . Linearity of these dispersion relations has the consequence that all Fourier modes travel with a common speed, thereby producing traveling waves of unchanging form. The simplest quadratic dispersion relation,  $\omega(k) = k^2$ , appears in the free space *Schrödinger equation*

$$i u_t = u_{xx}, \quad (2.4)$$

which is fundamental to quantum mechanics, [48]. The linear *beam equation*

$$u_{tt} + u_{xxxx} = 0, \quad (2.5)$$

which models small vibrations of a thin elastic beam, has bidirectional quadratic dispersion:  $\omega(k) = \pm k^2$ . The third order linear wave model

$$u_t + u_{xxx} = 0, \quad (2.6)$$

which is sometimes known as the *Airy partial differential equation*, since it admits solutions in terms of Airy functions, [39], or, alternatively, the *linear Korteweg–de Vries equation*, has cubic dispersion relation  $\omega(k) = k^3$ .

A fertile source of interesting wave models is the free boundary problem for water waves, meaning the dynamics of an incompressible, irrotational fluid under gravity. Let

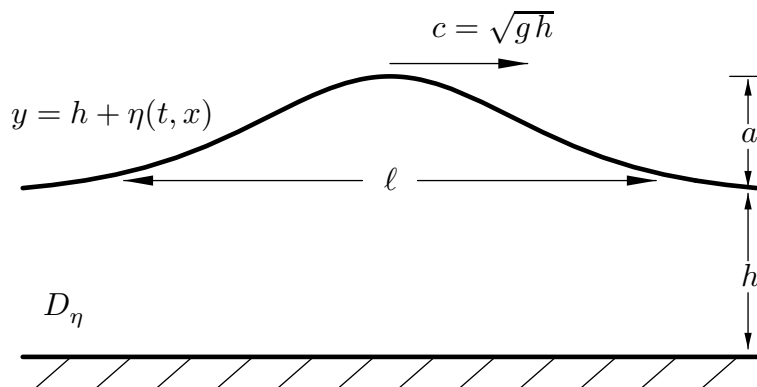


**Figure 1.** Water Waves.

us review, following [7, 37, 53], the derivation of models in the shallow water regime. For simplicity, we restrict our attention to two-dimensional flow, with  $x$  indicating the horizontal coordinate and  $y$  the vertical. (See [54] for the deep water regime, and [7, 36] for extensions to three-dimensional models.)

Suppose that the water sits on a flat, impermeable horizontal bottom, which we take as  $y = 0$ , and has undisturbed depth  $h$ . We assume further that the surface elevation at time  $t$  is the graph of a single-valued function

$$y = h + \eta(t, x), \quad (2.7)$$

i.e., there is no wave overturning. The periodic problem of interest here takes  $\eta$  to be a periodic function of  $x$  with mean 0, while, in contrast, solitary waves require  $\eta(t, x) \rightarrow 0$  as  $|x| \rightarrow \infty$ . The motion of the fluid is prescribed by the velocity potential  $\phi(t, x, y)$ , which is defined within the domain occupied by the fluid  $D_\eta = \{0 < y < h + \eta(t, x)\}$ ; see Figure 1. In the absence of surface tension, the free boundary problem governing the dynamical evolution of the water is then given by

$$\left. \begin{aligned} \phi_t + \frac{1}{2} \phi_x^2 + \frac{1}{2} \phi_y^2 + g\eta &= 0, \\ \eta_t &= \phi_y - \eta_x \phi_x, \\ \phi_{xx} + \phi_{yy} &= 0, \\ \phi_y &= 0, \end{aligned} \right\} \begin{aligned} y &= h + \eta(t, x), \\ 0 < y &< h + \eta(t, x), \\ y &= 0, \end{aligned} \quad (2.8)$$

in which  $g$  is the gravitational constant. As shown in Whitham, [53; §13.4], the dispersion relation for the linearized water wave system, obtained by omitting the nonlinear terms from the free surface conditions, is

$$\omega(k)^2 = gk \tanh(hk). \quad (2.9)$$

In the shallow water regime, one introduces the rescaling

$$x \mapsto \ell x, \quad y \mapsto hy, \quad t \mapsto \frac{\ell}{c} t, \quad \eta \mapsto a\eta, \quad \phi \mapsto \frac{ga\ell}{c} \phi, \quad (2.10)$$

in which  $\ell$  represents a typical wave length,  $h$  the undisturbed depth,

$$c = \sqrt{gh} \quad (2.11)$$

the leading order wave speed, and  $a$  the wave amplitude. Substituting (2.10) into the free boundary value problem (2.8), one formally solves the resulting rescaled Laplace equation for the potential  $\phi(t, x, y)$ , as a power series in the vertical coordinate  $y$ , in terms of the horizontal velocity  $u(t, x) = \phi_x(t, x, \theta)$  at a fraction  $0 \leq \theta \leq 1$  of the undisturbed depth  $h$ . Substituting the result into the free boundary conditions results in a system of equations of Boussinesq type, which, is then truncated to, say, first order in the small parameters

$$\alpha = \frac{a}{h}, \quad \beta = \frac{h^2}{\ell^2}, \quad (2.12)$$

representing the ratio of undisturbed depth to height of the wave, and the square of the ratio of height to wave length. We are interested in the regime of long waves in shallow water, in which both  $\alpha$  and  $\beta$  are small, but of comparable magnitudes. As in [7, 11, 37], the resulting *Boussinesq systems* are all of the general form

$$\begin{aligned} \eta_t + u_x + \alpha(\eta u)_x + \beta(a u_{xxx} - b \eta_{xxt}) &= 0, \\ u_t + \eta_x + \alpha u u_x + \beta(c \eta_{xxx} - d u_{xxt}) &= 0, \end{aligned} \quad (2.13)$$

where the parameters  $a, b, c, d$ , depend on the depth, and are subject to the physical constraints

$$a + b = \frac{1}{6}(3\theta^2 - 1), \quad c + d = \frac{1}{2}(1 - \theta^2), \quad a + b + c + d = 1. \quad (2.14)$$

The particular system

$$u_t + \eta_x + \alpha u u_x = 0, \quad \eta_t + u_x + \alpha(\eta u)_x + \frac{1}{3}\beta u_{xxx} = 0, \quad (2.15)$$

valid for  $\theta = 1$ , i.e., on the free surface, was derived by Whitham, [52], and Broer, [14], and shown to be completely integrable (in fact, tri-Hamiltonian) by Kaup, [28], and Kupershmidt, [29]. Bona, Chen, and Saut, [8], subsequently found that this system is, in fact, linearly ill-posed — although the question of nonlinear ill-posedness is, apparently, still open. The corresponding second order models can found in [7, 37].

The second stage is to restrict the bidirectional Boussinesq system (2.14) to a submanifold of approximately unidirectional solutions, building on the usual factorization of the second order wave equation (2.3) into right- and left-moving waves. Substituting the right-moving ansatz

$$\eta = u + \frac{1}{4}\alpha u^2 + \left(\frac{1}{2}\theta^2 - \frac{1}{3}\right)\beta u_{xx} + \dots \quad (2.16)$$

and truncating to first order reduces the Boussinesq system to the *Korteweg–de Vries equation*

$$u_t + u_x + \frac{3}{2}\alpha u u_x + \frac{1}{6}\beta u_{xxx} = 0, \quad (2.17)$$

for unidirectional propagation of long waves in shallow water. In the long wave regime,  $\beta \ll 1$ , the nonlinear effect is negligible, and the equation reduces to the linear equation

$$u_t + u_x + \frac{1}{6}\beta u_{xxx} = 0, \quad (2.18)$$

which in turn can be mapped to the third order Airy equation (2.6) by passing to a moving coordinate frame and then rescaling. Alternatively, since to leading order  $u_t \approx -u_x$ , one

can replace the third derivative term,  $u_{xxx} \approx -u_{xxt}$ , leading to the *RLW/BBM model*, [1, 42],

$$u_t + u_x + \frac{3}{2}\alpha u u_x - \frac{1}{6}\beta u_{xxt} = 0. \quad (2.19)$$

Observe that both first order models (2.17, 19) are independent of the depth parameter  $\theta$ , which only appears in the second and higher order terms in  $\alpha, \beta$ . Inverting the unidirectional constraint (2.16) leads to the same Korteweg–deVries equation and RLW/BBM equations for the surface elevation  $\eta$ . Again, this is only true up to first order, and the higher order terms are slightly different, [37]. Since the preceding unidirectional models do not admit the exact water wave dispersion relation (2.9), Whitham, [52], proposed the alternative model

$$u_t + L[u] + \frac{3}{2}\alpha u u_x = 0, \quad (2.20)$$

in which the Fourier integral operator

$$L[u] = \frac{1}{2\pi} \int_{-\infty}^{\infty} \int_{-\infty}^{\infty} \omega(k) e^{ik(x-\xi)} u(t, \xi) d\xi dk$$

exactly reproduces the rescaled water wave dispersion relation given by (2.9) when  $g = h = 1$ . However, Benjamin et. al., [1], argue that the linear dispersion in Whitham’s model is insufficiently strong to counteract the tendency to shock formation.

Let us also list a few important integrable nonlinear evolution equations, from a variety of physical sources. The *nonlinear Schrödinger equation*

$$i u_t = u_{xx} + |u|^2 u \quad (2.21)$$

arises in nonlinear optics as well as in the modulation theory for water waves, [54, 56]. Its linearization has quadratic dispersion relation  $\omega(k) = k^2$ . Integrability was established by Zakharov and Shabat, [57], and the fact that it admits localized soliton solutions that preserve their shape under collision plays an important role in transmission of signals through optical fibers, [25]. The integrable *Benjamin–Ono equation*

$$u_t + u u_x + \mathcal{H}[u_{xx}] = 0, \quad (2.22)$$

in which  $\mathcal{H}$  is the *Hilbert transform*, given by the Cauchy principal value integral

$$\mathcal{H}[u] = \int_{-\infty}^{\infty} \frac{u(\xi) d\xi}{\xi - x} \quad (2.23)$$

arises as a model for internal waves, [16]. Its linearization has quadratic dispersion relation  $\omega(k) = k^2 \operatorname{sign} k$ , which is the odd counterpart of the quadratic Schrödinger dispersion.

Another integrable model is the *Boussinesq equation*

$$u_{tt} = u_{xx} + \frac{3}{2}\alpha (u^2)_{xx} \pm \frac{1}{3}\beta u_{xxxx}, \quad (2.24)$$

also derived by Boussinesq from the water wave problem. While the Boussinesq equation admits waves propagating in both directions, it is not, in fact, equivalent to any of the bidirectional Boussinesq systems (2.13), and, indeed, its derivation from the water wave problem relies on the unidirectional hypothesis. The plus sign is the “bad Boussinesq”,

which is unstable, whereas the minus sign is the stable “good Boussinesq”. However, both versions admit solutions that blow up in finite time; see [33] for a detailed analysis of solutions to the periodic problem, and also [10, 44] for further results on stability and blow-up of solutions. An alternative, regularized version

$$u_{tt} = u_{xx} + \frac{3}{2} \alpha (u^2)_{xx} \pm \frac{1}{3} \beta u_{xxtt} \quad (2.25)$$

was subsequently investigated by Whitham, [53]. The integrable Boussinesq equation (2.24) and its regularization (2.25) were proposed as model for DNA dynamics by Scott and Muto, [35, 45]. The associated periodic boundary value problems can thus be viewed as a model for the dynamics of DNA loops, while individual DNA strands require suitably adapted boundary conditions at each end.

Let us summarize dispersion relations arising from water waves (in units so that  $g = h = 1$ ) and some of the more important shallow water models, rescaled so that  $\alpha = \beta = 1$ . In the first three cases, taking the positive square root corresponds to right moving waves. The final column lists their leading order asymptotics (omitting constant multiples) at large wave number.

### Shallow Water Dispersion Relations

Water waves	$\sqrt{k \tanh k} \operatorname{sign} k$	$ k ^{1/2} \operatorname{sign} k$
Boussinesq system, Regularized Boussinesq equation	$\frac{k}{\sqrt{1 + \frac{1}{3}k^2}}$	$\operatorname{sign} k$
Boussinesq equation	$k \sqrt{1 + \frac{1}{3}k^2}$	$k^2 \operatorname{sign} k$
Korteweg–deVries	$k - \frac{1}{6}k^3$	$k^3$
RLW/BBM	$\frac{k}{1 + \frac{1}{6}k^2}$	$k^{-1}$

### 3. Linear Dispersion in Periodic Domains.

In general, let  $L$  be a scalar, constant coefficient (integro-)differential operator with purely imaginary Fourier transform  $\widehat{L}(k) = i\varphi(k)$ . The associated scalar evolution equation

$$\frac{\partial u}{\partial t} = L[u] \quad (3.1)$$



has real dispersion relation

$$\omega(k) = i\widehat{L}(k) = -\varphi(k).$$

We subject (3.1) to periodic boundary conditions on the interval  $-\pi \leq x \leq \pi$ , (or, equivalently, work on the unit circle:  $x \in S^1$ ) with initial conditions

$$u(0, x) = f(x). \quad (3.2)$$

To construct the solution, we expand the initial condition in a Fourier series:

$$f(x) \sim \sum_{k=-\infty}^{\infty} c_k e^{ikx}, \quad \text{where} \quad c_k = \frac{1}{2\pi} \int_{-\pi}^{\pi} f(x) e^{-ikx} dx. \quad (3.3)$$

The solution to the periodic initial-boundary value problem then has time-dependent Fourier series

$$u(t, x) \sim \sum_{k=-\infty}^{\infty} c_k e^{i[kx - \omega(k)t]}. \quad (3.4)$$

In particular, the *fundamental solution*  $u = F(t, x)$  takes a delta function as its initial data,  $u(0, x) = \delta(x)$ , and hence has the following Fourier expansion

$$F(t, x) \sim \frac{1}{2\pi} \sum_{k=-\infty}^{\infty} e^{i[kx - \omega(k)t]}. \quad (3.5)$$

The solution (3.4) to the general periodic initial-boundary value problem (3.1–2) can then be rewritten as a convolution integral with the fundamental solution:

$$u(t, x) = \int_{-\pi}^{\pi} F(t, x - \xi) f(\xi) d\xi. \quad (3.6)$$

The following result underlies the dispersive quantization effect for equations with “integral polynomial” dispersion relations.

**Definition 3.1.** A polynomial  $P(k) = c_m k^m + \dots + c_1 k + c_0$  will be called *integral* if all its coefficients are integers:  $c_j \in \mathbb{Z}$ ,  $j = 0, \dots, m$ .

**Theorem 3.2.** *Suppose that the dispersion relation of the evolution equation (3.1) is a multiple of an integral polynomial:*

$$\omega(k) = \lambda P(k), \quad \text{for some} \quad 0 \neq \lambda \in \mathbb{R}.$$

Let  $\beta = 2\pi/\lambda$ . Then at every rational time  $t = \beta p/q$ , with  $p$  and  $0 \neq q \in \mathbb{Z}$ , the fundamental solution (3.5) is a linear combination of  $q$  periodically extended delta functions concentrated at the rational nodes  $x_j = 2\pi j/q$  for  $j \in \mathbb{Z}$ .

As in [38], this result is an immediate consequence of the following well-known lemma:

**Lemma 3.3.** *Let  $0 < q \in \mathbb{Z}$ . The coefficients of a complex Fourier series (3.3) are  $q$ -periodic in their indices, so  $c_{k+q} = c_k$  for all  $k$ , if and only if the series represents a linear combination of the  $q$  periodically extended delta functions concentrated at the rational nodes  $x_j = 2\pi j/q$  for  $j \in \mathbb{Z}$ :*

$$f(x) = \sum_{-\frac{1}{2}q < j \leq \frac{1}{2}q} a_j \delta\left(x - \frac{2\pi j}{q}\right),$$

for certain  $a_0, \dots, a_{q-1} \in \mathbb{C}$ .

Applying Theorem 3.2 to the superposition formula (3.6) produces the following intriguing corollary:

**Corollary 3.4.** *Under the assumptions of Theorem 3.2, at a rational time  $t = \beta p/q$ , the solution profile to the periodic initial-boundary value problem is a linear combination of  $\leq q$  translates of its initial data  $u(0, x) = f(x)$ , i.e.,*

$$u\left(\frac{\beta p}{q}, x\right) = \sum_{-\frac{1}{2}q < j \leq \frac{1}{2}q} a_j \left(\frac{\beta p}{q}\right) f\left(x - \frac{2\pi j}{q}\right).$$

In the case of the ‘‘Riemann problem’’, the initial data is the unit step function:

$$u(0, x) = f(x) = \sigma(x) = \begin{cases} 0, & -\pi < x < 0, \\ 1, & 0 < x < \pi. \end{cases} \quad (3.7)$$

Under the assumption that the dispersion relation is odd,  $\omega(-k) = -\omega(k)$ , the Fourier expansion of the resulting solution is

$$u^*(t, x) \sim \frac{1}{2} + \frac{2}{\pi} \sum_{j=0}^{\infty} \frac{\sin[(2j+1)x - \omega(2j+1)t]}{2j+1}, \quad (3.8)$$

whose spatial derivative is the difference of two translates of the fundamental solution, namely,  $\partial u^*/\partial x = F(t, x) - F(t, x - \pi)$ . Non-odd dispersion relations produce complex solutions, whose real part is given by the more complicated expression

$$\frac{1}{2} + \frac{1}{\pi} \sum_{j=0}^{\infty} \frac{\sin[(2j+1)x - \omega(2j+1)t] + \sin[(2j+1)x + \omega(-2j-1)t]}{2j+1}. \quad (3.9)$$

At the end of the paper, we display graphs of the solution (3.8) at some representative times, for various *odd* dispersion relations, most of which are associated with water waves models. The figures are ordered by their asymptotic order  $\alpha$  at large wave number:  $\omega(k) = O(|k|^\alpha)$  as  $|k| \rightarrow \infty$ . We did not use numerical integration to obtain these plots; rather, they were produced in MATHEMATICA by summing the first 150 terms in the Fourier series (3.8), which was adequate to capture the essential detail. (In all the cases we looked at, summing the first 1000 terms does not appreciably change the solution graphs.) In some plots, a tiny residual Gibbs effect can be seen at the jump discontinuities. By comparing the various profiles, we conclude that the qualitative behavior of the solution (3.8) depends

crucially on the asymptotic behavior of the dispersion relation  $\omega(k)$  for large wave number. However, a full understanding of the various qualitative behaviors cannot be gleaned from these few static solution profiles, and so the reader is strongly encouraged to watch the corresponding movies that have been posted at

<http://www.math.umn.edu/~olver/mvdq1.html>

Each movie shows the dynamical behavior of the solutions (3.8) for various dispersion relations over a range of times; the associated figures at the end of the paper are selected frames extracted from the corresponding movie. In some cases, the solution evolves at a glacially slow pace, so a representative collection of sub-movies are posted. Again, we emphasize that all dispersion relations used in the figures and movies are odd functions of  $k$ . More general dispersion relations, which produce complex oscillatory solutions whose real part is given by the more complicated formula (3.9), exhibit additional qualitative features that we will investigate more thoroughly elsewhere.

Here is an attempt to convey in words the behaviors that can be observed in the movies, but are sometimes less evident in the plots appearing at the end of the paper. In all cases considered, the large wave number asymptotics is fixed by a certain power of the wave number:

$$\omega(k) \sim |k|^\alpha \quad \text{as} \quad |k| \rightarrow \infty. \quad (3.10)$$

In our experiments, the overall qualitative behavior seems to be entirely determined by the asymptotic exponent  $\alpha$ , although the intricate details of the solution profile do depend upon the particularities of the dispersion relation. As  $\alpha$  varies, there is a continual change from one type of qualitative behavior to the next. Over the range  $-\infty < \alpha < \infty$ , there appear to be five main regions which are roughly demarcated as follows.

- $\alpha \leq 0$ . *Large scale oscillations*: The two initial discontinuities, at 0 and  $\pi$ , remain stationary and begin to produce oscillating waves moving to the left. After this initial phase, the solution settles into what is essentially a stationary up and down motion, with very gradually accumulating waviness superimposed. Two examples are the dispersion relations associated with the RLW/BBM equation (2.19), with  $\alpha = -1$ , shown in Figure 2, and the regularized Boussinesq equation (2.25) as well as some versions of the Boussinesq system (2.13), for which  $\alpha = 0$ , shown in Figure 3. Interestingly, the former becomes wavier sooner, whereas in the latter, even after time  $t = 1000$ , the smaller scale oscillations are still rather coarse, and numerical limitations prevented us from following it far enough to see very high frequency oscillations appear.
- $0 < \alpha < 1$ . *Dispersive oscillations*: Each of the two initial discontinuities changes into a slowly moving “seed” that continually spawns a right-moving oscillatory wave train. After a while, the wave train emanating from one seed interacts with the other, and the seeds follow along these increasingly rapid oscillations. Much later, the solution has assumed a slightly fractal wave form superimposed over a slowly oscillating ocean, similar to ripples on a swelling sea that moves up and down while gradually changing form. Examples include the full water wave dispersion relation, plotted in Figure 4, and the square root dispersion graphed in Figure 5. Observe

that both have the same large wave number asymptotics, and the corresponding solutions have very similar qualitative behavior, while differing in their fine details.

- $\alpha = 1$ . *Slowly varying traveling waves*: As  $\alpha$  approaches 1, the oscillatory waves acquire an increasingly noticeable motion to the right. Indeed, if the dispersion relation is exactly linear,  $\omega(k) = k$ , the solution is a pure traveling wave  $u(t, x) = f(x - t)$ , that moves unchanged with unit speed. Having asymptotically, but not exactly linear, dispersion relation, superimposes slowly varying oscillations on top of the traveling wave. An example appears in Figure 6, based on the asymptotically linear dispersion relation  $\omega(k) = \sqrt{|k(k+1)|} \operatorname{sign} k$  associated with, for example, the equation<sup>†</sup>

$$u_{tt} = u_{xx} + i u_x. \quad (3.11)$$

- $1 < \alpha < 2$ . *Oscillatory becoming fractal*: In this range, each of the initial discontinuities produces an oscillatory wave train propagating to the right. After the wave train encounters the other discontinuity, the oscillations become increasingly rapid over the entire interval, and, after a while, the entire solution acquires a fractal profile, that displays an overall motion to the right while its small scale features vary rapidly and seemingly chaotically. An example is provided in Figure 7, based on the dispersion relation  $\omega(k) = |k|^{3/2} \operatorname{sign} k$  corresponding to the equation

$$u_{tt} = -i u_{xxx}. \quad (3.12)$$

- $\alpha \geq 2$ . *Fractal/quantized*: Once  $\alpha$  reaches 2, the solution exhibits the fractalization/quantization phenomenon, which provably happens when the dispersion relation is an integral polynomial, e.g.,  $\omega(k) = k^m$  where  $2 \leq m \in \mathbb{Z}$ . In such cases, Theorem 3.2 implies that the solution quantizes at rational times, meaning that, when  $t = \beta p/q$  it is piecewise constant on intervals of length  $2\pi/q$ , and, as proved by Oskolkov, [41], continuous but nowhere differentiable at irrational times. For non-polynomial dispersion with integral asymptotic exponent  $2 \leq \alpha \in \mathbb{Z}$ , most frames in the movie show a fractal profile, but occasionally the profile will abruptly quantize, with jump discontinuities punctuating noticeably less fractal subgraphs. We presume that, as in the polynomial case, the times at which the solution (approximately) quantizes are densely embedded in the times at which it has a continuous, fractal profile. However, a rigorous proof of this observation appears to be quite difficult, requiring delicate Fourier estimates. Examples include the linearized Korteweg–deVries equation (2.6), and linearized Benjamin–Ono equation (2.22), both of which precisely quantize, as seen in Figures 8 and 11, and the linearization of the integrable Boussinesq equation (2.24), which appears to do so approximately, as in Figure 9. On the other hand, if  $2 \leq \alpha \notin \mathbb{Z}$  is not an integer (or at least not very close to an integer), only fractal solution profiles are observed; see Figure 10 for the case  $\omega(k) = |k|^{5/2} \operatorname{sign} k$  corresponding to the

---

<sup>†</sup> The figure can be viewed as graphing the real part of the right-moving component of the solution to the periodic Riemann initial value problem.

equation

$$u_{tt} = i u_{xxxxx}. \quad (3.13)$$

Observe that, as an immediate consequence of Corollary 3.4, for integral polynomial dispersion relations, and, presumably, more general relations in this region, the quantization effect persists under the addition of noise to the initial data, although the small jumps at rational numbers with large denominators would be overwhelmed by the noise, whereas at irrational steps one ends up with a “noisy fractal”.

Let us outline a justification of our observation that the quantization and fractalization phenomena hold for dispersion relations that are asymptotically polynomial at large wave number. Assume that

$$\omega(k) \sim \lambda P(k) + O(k^{-1}) \quad \text{as} \quad |k| \longrightarrow \infty, \quad (3.14)$$

where  $0 \neq \lambda \in \mathbb{R}$ , and  $P(k)$  is an integral polynomial. Let us rewrite the corresponding complex Fourier series solution in the form

$$u(t, x) = b_0 + \sum_{\substack{k=-\infty \\ k \neq 0}}^{\infty} \frac{b_k}{k} e^{i[kx - \omega(k)t]} = b_0 + \sum_{\substack{k=-\infty \\ k \neq 0}}^{\infty} \frac{b_k}{k} e^{i[kx - p(k)t]} + \sum_{\substack{k=-\infty \\ k \neq 0}}^{\infty} r_k e^{ikx},$$

We assume that the coefficients  $b_k$ , which are prescribed by the initial data, are uniformly bounded,  $|b_k| \leq M$ , as is the case with the step function. With this assumption,  $r_k = O(k^{-2})$ , and hence the final series represents a uniformly and absolutely convergent Fourier series, whose sum is a continuous function. Thus, the discontinuities of  $u(t, x)$  will be determined by the initial series, which, by Theorem 3.2, exhibits jump discontinuities and quantization at rational times. We conclude that solutions to linear equations with such asymptotically integral polynomial dispersion relations will exhibit quantization at the rational times  $t = \beta p/q$ , where  $\beta = 2\pi/\lambda$ . A rigorous proof of fractalization at irrational times will require a more detailed analysis.

A similar argument explains why, when the asymptotic exponent  $\alpha < 0$ , the discontinuities in the solution remain (almost) stationary. Formally, suppose  $\omega(k) = |k|^\alpha \mu(k)$ , where  $\alpha < 0$  and  $\mu(k) = O(1)$ . Then, the Fourier series solution has the form

$$u(t, x) = b_0 + \sum_{\substack{k=-\infty \\ k \neq 0}}^{\infty} \frac{b_k}{k} e^{i[kx - \omega(k)t]} = b_0 + \sum_{\substack{k=-\infty \\ k \neq 0}}^{\infty} \frac{b_k}{k} e^{ikx} [1 - it |k|^\alpha \mu(k)].$$

Again, assuming that the coefficients  $b_k$  are uniformly bounded, the remainder terms are of order  $k^{-1+\alpha}$  with  $\alpha < 0$ , and hence represent a uniformly convergent series whose sum is continuous. We conclude that the discontinuities of  $u(t, x)$  are completely determined by those of the leading term, which are stationary.

Finally, in Figure 12 we display graphs of the temporal evolution of the solution at the origin,  $u(t, 0)$ , for a representative subset of the dispersion relations we’ve considered. In the first two figures, for the RLW/BBM and water wave dispersion, we graph on the long time interval  $0 \leq t \leq 100$ , while in the other plots, the time interval is  $0 \leq t \leq 2\pi$ .

When the asymptotic power (3.10) governing the high wave number dispersion satisfies  $\alpha \leq 1$ , the time plot appears smooth. Following the non-rigorous analysis presented in [2; Section 2], for  $\alpha \geq 1$ , the fractal dimension of the time plot should be  $2 - 1/(2\alpha)$ . This seems correct as stated when  $\alpha \geq 2$ , as these plots become increasingly fractal with increasing asymptotic dispersion power  $\alpha$ . However, for  $\alpha$  near 1, the plot appears to be initially smooth for a short time, which is followed by the appearance of increasingly rapid oscillations. After some further time has elapsed, the graph eventually assumes a fractal form.

#### 4. Fractalization and Quantization in Nonlinear Systems.

In this final section, we turn our attention to the nonlinear regime. Basic numerical techniques will be employed to approximate the solutions to the Riemann initial value problem on a periodic domain. While we do not have any rigorous theoretical results to justify the resulting observations, our numerical studies strongly indicate that the variety of qualitative solution features observed in the underlying linear problem persist, at the very least, into the weakly nonlinear regime. In particular, the fractalization and quantization of solutions to the Airy evolution equation are observed in the numerical solutions to the both the integrable Korteweg–deVries equation and its non-integrable quartic counterpart. Similar phenomena have been found in nonlinear Schrödinger equations, but these will be reported on elsewhere.

Our numerical algorithms are based on a standard operator splitting method, [26]. Consider the initial value problem for an evolution equation

$$u_t = K[u], \quad u(t_0, x) = u_0(x), \quad (4.1)$$

where  $K$  is a differential operator (linear or nonlinear) in the spatial variable. Here the system is always supplemented by periodic boundary conditions, but the numerical scheme is of complete generality. Assuming the basic existence and uniqueness of solutions to the initial value problem, at least over a certain time interval  $0 < t < t_*$ , we denote the resulting solution to (4.1), i.e., the induced flow, by

$$u(t, \cdot) = \Phi_K(t) u_0.$$

Operator splitting relies on writing the spatial operator as a sum

$$K[u] = L[u] + N[u] \quad (4.2)$$

of two simpler operators, which can each be more readily solved numerically. In all cases treated here,  $L[u]$  represents the linear part of the evolution equation (4.1), while the nonlinear terms appear in  $N[u]$ . For example, writing the Korteweg–deVries equation in the reduced form<sup>†</sup>

$$u_t = K[u] = -u_{xxx} + u u_x, \quad (4.3)$$

---

<sup>†</sup> The model version (2.17) can be changed into the reduced form by applying a combination of scaling and Galilean boost.

we split the right hand side into the sum of the linear part  $L[u] = -u_{xxx}$ , with cubic dispersion, and the nonlinear part given by the *inviscid Burgers' operator*  $N[u] = u u_x$ .

For numerical purposes, we are interested in approximating the solution  $u_n(x) = u(t_n, x)$  at the mesh points  $0 = t_0 < t_1 < t_2 < \dots$  which, for simplicity, we assume to be equally spaced, with  $\Delta t = t_n - t_{n-1}$  fixed. (Of course, we will also discretize the spatial variable.) We use  $u_n^\Delta(t_n, x) = u_n^\Delta(x)$  to denote the numerical approximation to the solution to the original evolution equation at times  $t_n = n\Delta t$ , which is obtained by successively applying the flows  $\Phi_L$  and  $\Phi_N$  corresponding, respectively, to the linear and nonlinear parts in the splitting (4.2). The simplest splitting algorithm is the *Godunov scheme*:

$$u_{n+1}^\Delta = \Phi_L(\Delta t)\Phi_N(\Delta t)u_n^\Delta, \quad n = 0, 1, 2, \dots, \quad u_0^\Delta = u_0. \quad (4.4)$$

In favorable situations, for a suitable choice of norm and appropriate conditions on the initial data, it can be proved that the Godunov scheme is first order convergent:

$$\|u_n^\Delta(x) - u(t_n, x)\| = O(\Delta t), \quad \text{as } \Delta t \rightarrow 0.$$

The convergence can be improved to second order by use of the *Strang splitting scheme*:

$$u_{n+1}^\Delta = \Phi_N\left(\frac{1}{2}\Delta t\right)\Phi_L(\Delta t)\Phi_N\left(\frac{1}{2}\Delta t\right)u_n^\Delta, \quad n = 0, 1, 2, \dots, \quad u_0^\Delta = u_0. \quad (4.5)$$

In this case,

$$\|u_n^\Delta(x) - u(t_n, x)\| = O(\Delta t^2), \quad \text{as } \Delta t \rightarrow 0,$$

again under appropriate assumptions. In our numerical experiments, the results of the Godunov and Strang splitting are very similar, and so we only display the Godunov versions in the figures.

In particular, to solve the initial value problem for the Korteweg–deVries equation (4.3), we apply the Godunov splitting scheme (4.4) to its linear and nonlinear parts

$$u_t = L[u] = -u_{xxx}, \quad u_t = N[u] = \partial_x\left(\frac{1}{2}u^2\right), \quad (4.6)$$

each of which is subject to periodic boundary conditions. Periodicity and discretization of the spatial variable enables us to apply the fast Fourier transform (FFT) to exactly solve the discretized linear equation. On the other hand, the nonlinear inviscid Burgers' equation is first written in conservative form as above. As in the linear case, we use FFT to write the numerical approximation in the form of a Fourier series, apply convolution to square the numerical solution, and then differentiate by multiplication by the frequency variable. The resulting system of ordinary differential equations is mildly stiff, and is integrated by applying the Backward Euler Method based on the implicit midpoint rule, using fixed point iteration to approximate the solution to the resulting nonlinear algebraic system to within a prescribed tolerance. Because the time step is small, difficulties with the formation of shock waves and other discontinuities do not complicate the procedure.

Our results, at rational and irrational times, are plotted in Figures 13 and 14. These clearly suggest the presence of both quantization and fractalization phenomena in the nonlinear system. It is striking that these appear, not just, as one might expect, in the weakly nonlinear regime, but in a fully nonlinear framework in which the coefficients of both

the linear and nonlinear terms in (4.3) have comparable magnitude. Indeed, recent results of Erdoğan, Tzirakis, and Zharnitsky, [18], imply that, for periodic boundary conditions, the temporal evolution of high frequency data for the Korteweg–deVries equation and other nonlinear water wave models is nearly linear over long time intervals. So, while it may happen that these effects may eventually be overcome by the nonlinearity, any serious investigation will require very accurate long time numerical integration schemes. The corresponding movies have been posted at

<http://www.math.umn.edu/~olver/mvdqn.html>

Our numerical results are also in agreement with a theorem of Erdoğan and Tzirakis, [17; Corollary 1.5], that, when the initial data  $u(0, \cdot)$  lies in the Sobolev space  $H^s$  with  $s > -\frac{1}{2}$ , then the difference between solutions of the Korteweg–deVries equation and its linearization can be controlled, meaning that the difference lies in  $H^r$  for any  $r < \min\{3s + 1, s + 1\}$ , and has at most polynomially growing  $H^r$  norm.

To verify that these phenomena are not restricted to integrable models such as the Korteweg–deVries equation, in Figures 15 and 16 we plot the solution to the non-integrable *quartic Korteweg–deVries equation*

$$u_t = -u_{xxx} + u^3 u_x = -u_{xxx} + \left(\frac{1}{4} u^4\right)_x. \quad (4.7)$$

The numerical solution algorithm is again based on Godunov splitting, using the same Fourier-based algorithms to integrate the individual linear and nonlinear parts.

Keep in mind that the coefficients in both the Korteweg–deVries and quartic Korteweg–deVries equations can be rescaled to any convenient non-zero values, and thus quantization and fractalization of the solution can be expected to appear in any version, perhaps with the overall magnitude of the effect governed by the relative size of the initial discontinuities. Thus, the Talbot effect appears to be rather robust, and hence of importance to a wide range of linear and nonlinear dispersive equations on periodic domains.

## 5. Further Directions.

We conclude by listing a few of the possibly fruitful directions for further research.

- Our numerical integration schemes are fairly crude, and it would be worth implementing more sophisticated algorithms. See [58] for a recent survey on the numerics of dispersive partial differential equations. In the linear case, the complicated behaviors exhibited by the (partial) Fourier series sums would serve as a good testing ground for the application of numerical methods for dispersive waves to rough data.
- While the explicit formulas for the solutions are rather simple Fourier series, the amazing variety of observed behaviors, solution profiles, and fascinating spatial and temporal patterns indicates that formulation of theorems and rigorous proofs will be very challenging. Progress may well rely on delicate estimates, of the type used in the analysis of number-theoretic exponential sums of Gauss and Weyl type, [51]. One is also reminded of Bourgain’s celebrated analysis of the periodic



problems for the nonlinear Schrödinger and Korteweg–deVries equations, [12, 13], that involves similarly subtle number-theoretic analysis.

- Zabusky and Kruskal’s numerical experimentations that led to the discovery of the soliton were motivated by the fact that the Korteweg–deVries and Boussinesq equations are continuum limits of the nonlinear mass-spring chains, whose surprising lack of thermalization came to light in the seminal work of Fermi, Pasta, and Ulam, [19]. It would be interesting to see how the foregoing dispersive effects might be manifested in the original Fermi–Pasta–Ulam chains when the initial displacement includes a sharp transition.
- An interesting and apparently difficult question is to determine the fractal dimension of the graphs of solutions at fixed times that are given by such slowly converging Fourier series. The wide variety of individual space plots in the accompanying figures indicates that this is considerably more subtle than the Fourier series that were rigorously analyzed by Chamizo and Córdoba, [15], or those of Weierstrass–Mandelbrot form that were investigated by Berry and Lewis, [5]. Indeed, for fixed  $t$ , all of our series have the same slow  $O(1/k)$  rate of decay of their Fourier coefficients, and hence the fractal nature of their graphs depends essentially on the detailed dispersion relation asymptotics. Further, when the large wave number asymptotic power is in the range  $1 < \alpha < 2$ , the graphs appear to be (mostly) smooth over some initial time interval, then increasingly oscillatory, only later apparently achieving a fractal nature. Using Besov space methods, Rodnianski, [43], rigorously proves that the graphs of real and imaginary parts of rough solutions to the linear Schrödinger equation have fractal dimension  $\frac{3}{2}$  at a dense subset of irrational times, reconfirming some of Berry’s observations, [2]. We do not know how difficult it would be to extend Rodnianski’s techniques to more general dispersion relations.
- We have concentrated on the periodic boundary value problem for linearly dispersive wave equations. The behavior under other boundary conditions, e.g.,  $u(t, 0) = u_x(t, 0) = u(t, 2\pi) = 0$ , is not so clear because, unlike the Schrödinger equation, these boundary value problems are not naturally embedded in the periodic version. Fokas and Bona, [9, 20, 21], have developed a new solution technique for initial-boundary value problems for linear and integrable nonlinear dispersive partial differential equations based on novel complex integral representations. It would be instructive to investigate how the effects of the dispersion relation in the periodic and other problems are manifested in this approach.
- Another important direction would be to extend our analysis to linearly dispersive equations in higher space dimensions. Berry, [2], gives a non-rigorous argument that, at least for the linearized Schrödinger equation, a fractal Talbot effect persists for higher dimensional boundary value problems. Other important examples worth investigating include the integrable Kadomtsev–Petviashvili (KP) and Davey–Stewartson equations, [16], and non-integrable three-dimensional surface wave models found in [7, 36].

*Acknowledgments:* We'd like to thank Michael Berry, Jerry Bona, Adrian Diaconu, Dennis Hejhal, Svitlana Mayboroda, and Konstantin Oskolkov for supplying references and helpful advice. We also thank the anonymous referees for helpful and thought-provoking comments.

## References

- [1] Benjamin, T.B., Bona, J.L., and Mahony, J.J., Model equations for long waves in nonlinear dispersive systems, *Phil. Trans. Roy. Soc. London A* **272** (1972), 47–78.
- [2] Berry, M.V., Quantum fractals in boxes, *J. Phys. A* **29** (1996), 6617–6629.
- [3] Berry, M.V., and Bodenschatz, E., Caustics, multiply-reconstructed by Talbot interference, *J. Mod. Optics* **46** (1999), 349–365.
- [4] Berry, M.V., and Klein, S., Integer, fractional and fractal Talbot effects, *J. Mod. Optics* **43** (1996), 2139–2164.
- [5] Berry, M.V., and Lewis, Z.V., On the Weierstrass–Mandelbrot fractal function, *Proc. Roy. Soc. London A* **370** (1980), 459–484.
- [6] Berry, M.V., Marzoli, I., and Schleich, W., Quantum carpets, carpets of light, *Physics World* **14**(6) (2001), 39–44.
- [7] Bona, J.L., Chen, M., and Saut, J.–C., Boussinesq equations and other systems for small-amplitude long waves in nonlinear dispersive media. I. Derivation and linear theory, *J. Nonlinear Sci.* **12** (2002), 283–318.
- [8] Bona, J.L., Chen, M., and Saut, J.–C., Boussinesq equations and other systems for small-amplitude long waves in nonlinear dispersive media. II. The nonlinear theory, *Nonlinearity* **17** (2004), 925–952.
- [9] Bona, J.L., and Fokas, A.S., Initial-boundary-value problems for linear and integrable nonlinear dispersive partial differential equations, *Nonlinearity* **21** (2008), T195–T203.
- [10] Bona, J.L., and Sachs, R.L., Global existence of smooth solutions and stability of solitary waves for a generalized Boussinesq equation, *Commun. Math. Phys.* **118** (1988), 15–29.
- [11] Bona, J.L., and Smith, R., A model for the two-way propagation of water waves in a channel, *Math. Proc. Camb. Phil. Soc.* **79** (1976), 167–182.
- [12] Bourgain, J., Exponential sums and nonlinear Schrödinger equations, *Geom. Funct. Anal.* **3** (1993), 157–178.
- [13] Bourgain, J., Periodic Korteweg de Vries equation with measures as initial data, *Selecta Math.* **3** (1997), 115–159.
- [14] Broer, L.J.F., Approximate equations for long water waves, *Appl. Sci. Res.* **31** (1975), 377–395.
- [15] Chamizo, F., and Córdoba, A., Differentiability and dimension of some fractal Fourier series, *Adv. Math.* **142** (1999), 335–354.
- [16] Drazin, P.G., and Johnson, R.S., *Solitons: An Introduction*, Cambridge University Press, Cambridge, 1989.

- [17] Erdoğan, M.B., and Tzirakis, N., Global smoothing for the periodic KdV evolution, *Inter. Math. Res. Notes*, to appear.
- [18] Erdoğan, M.B., Tzirakis, N., and Zharnitsky, V., Nearly linear dynamics of nonlinear dispersive waves, *Physica D* **240** (2011), 1325–1333.
- [19] Fermi, E., Pasta, J., and Ulam, S., Studies of nonlinear problems. I., preprint, Los Alamos Report LA 1940, 1955; in: *Nonlinear Wave Motion*, A.C. Newell, ed., Lectures in Applied Math., vol. 15, American Math. Soc., Providence, R.I., 1974, pp. 143–156.
- [20] Fokas, A.S., *A Unified Approach to Boundary Value Problems*, CBMS–NSF Conference Series in Applied Math., vol. 78, SIAM, Philadelphia, 2008.
- [21] Fokas, A.S., and Spence, E.A., Synthesis, as opposed to separation, of variables, *SIAM Review* **54** (2012), 291–324.
- [22] Ford, K., Recent progress on the estimation of Weyl sums, in: *Modern Problems of Number Theory and its Applications: Current Problems, Part II*, V.N. Chubarikov and G.I. Arkhipov, eds., Mosk. Gos. Univ. im. Lomonosova, Mekh.-Mat. Fak., Moscow, 2002, pp. 48–66.
- [23] Hannay, J.H., and Berry, M.V., Quantization of linear maps on a torus — Fresnel diffraction by a periodic grating, *Physica* **1D** (1980), 267–290.
- [24] Hardy, G.H., and Littlewood, J.E., Some problems of Diophantine approximation. II. The trigonometric series associated with the elliptic  $\vartheta$ -functions, *Acta Math.* **37** (1914), 193–238.
- [25] Hasegawa, A., and Matsumoto, M., *Optical Solitons in Fibers*, Third Edition, Springer–Verlag, New York, 2003.
- [26] Holden, H., Karlsen, K.H., Risebro, N.H., and Tao, T., Operator splitting for the KdV equation, *Math. Comp.* **80** (2011), 821–846.
- [27] Kapitanski, L., and Rodnianski, I., Does a quantum particle know the time?, in: *Emerging Applications of Number Theory*, D. Hejhal, J. Friedman, M.C. Gutzwiller and A.M. Odlyzko, eds., IMA Volumes in Mathematics and its Applications, vol. 109, Springer Verlag, New York, 1999, pp. 355–371.
- [28] Kaup, D.J., A higher-order water-wave equation and the method for solving it, *Prog. Theor. Physics* **54** (1975), 396–408.
- [29] Kupershmidt, B.A., Mathematics of dispersive waves, *Commun. Math. Phys.* **99** (1985), 51–73.
- [30] Lax, P.D., Periodic solutions to the KdV equation, *Commun. Pure Appl. Math.* **28** (1975), 141–188.
- [31] Lax, P.D., and Levermore, C.D., The small dispersion limit of the Korteweg–deVries equation I, II, III, *Commun. Pure Appl. Math.* **36** (1983), 253–290, 571–593, 809–829.
- [32] Lax, P.D., Levermore, C.D., and Venakides, S., The generation and propagation of oscillations in dispersive initial value problems and their limiting behavior, in: *Important developments in soliton theory*, A.S. Fokas and V.E. Zakharov, eds., Springer–Verlag, Berlin, 1993, pp. 205–241.

- [33] McKean, H.P., Boussinesq’s equation on the circle, *Commun. Pure Appl. Math.* **34** (1981), 599–691.
- [34] McKean, H.P., and van Moerbeke, P., The spectrum of Hill’s equation, *Invent. Math.* **30** (1975), 217–274.
- [35] Muto, V., Soliton oscillations for DNA dynamics, *Acta Appl. Math.* **115** (2011), 5–15.
- [36] Nwogu, O., Alternative form of Boussinesq equations for nearshore wave propagation, *J. Waterway Port Coastal Ocean Eng.* **119** (1993), 618–638.
- [37] Olver, P.J., Hamiltonian perturbation theory and water waves, *Contemp. Math.* **28** (1984), 231–249.
- [38] Olver, P.J., Dispersive quantization, *Amer. Math. Monthly* **117** (2010), 599–610.
- [39] Olver, P.J., *Introduction to Partial Differential Equations*, Pearson Publ., Upper Saddle River, N.J., to appear.
- [40] Oskolkov, K.I., Schrödinger equation and oscillatory Hilbert transforms of second degree, *J. Fourier Anal. Appl.* **4** (1998), 341–356.
- [41] Oskolkov, K.I., A class of I.M. Vinogradov’s series and its applications in harmonic analysis, in: *Progress in Approximation Theory*, Springer Ser. Comput. Math., 19, Springer, New York, 1992, pp. 353–402.
- [42] Peregrine, D.H., Calculations of the development of an undular bore, *J. Fluid Mech.* **25** (1966), 321–330.
- [43] Rodnianski, I., Fractal solutions of the Schrödinger equation, *Contemp. Math.* **255** (2000), 181–187.
- [44] Sachs, R.L., On the blow-up of certain solutions of the “good” Boussinesq equation, *Appl. Anal.* **36** (1990), 145–152.
- [45] Scott, A.C., Soliton oscillations in DNA, *Phys. Rev. A* **31** (1985), 3518–3519.
- [46] Talbot, H.F., Facts related to optical science. No. IV, *Philos. Mag.* **9** (1836), 401–407.
- [47] Taylor, M., The Schrödinger equation on spheres, *Pacific J. Math.* **209** (2003), 145–155.
- [48] Thaller, B., *Visual Quantum Mechanics*, Springer–Verlag, New York, 2000.
- [49] Venakides, S., The zero dispersion limit of the Korteweg–deVries equation with nontrivial reflection coefficient, *Commun. Pure Appl. Math.* **38** (1985), 125–155.
- [50] Venakides, S., The zero dispersion limit of the Korteweg–deVries equation with periodic initial data, *Trans. Amer. Math. Soc.* **301** (1987), 189–225.
- [51] Vinogradov, I.M., *The Method of Trigonometrical Sums in the Theory of Numbers*, Dover Publ., Mineola, NY, 2004.
- [52] Whitham, G.B., Variational methods and applications to water waves, *Proc. Roy. Soc. London* **299A** (1967), 6–25.
- [53] Whitham, G.B., *Linear and Nonlinear Waves*, John Wiley & Sons, New York, 1974.
- [54] Yuen, H.C., and Lake, B.M., Instabilities of waves on deep water, *Ann. Rev. Fluid Mech.* **12** (1980), 303–334.
- [55] Zabusky, N.J., and Kruskal, M.D., Interaction of “solitons” in a collisionless plasma and the recurrence of initial states, *Phys. Rev. Lett.* **15** (1965), 240–243.

- [56] Zakharov, V.E., Stability of periodic waves of finite amplitude on the surface of a deep fluid, *J. Appl. Mech. Tech. Phys.* **2** (1968), 190–194.
- [57] Zakharov, V.E., and Shabat, A.B., A scheme for integrating the nonlinear equations of mathematical physics by the method of the inverse scattering problem. I, *Func. Anal. Appl.* **8** (1974), 226–235.
- [58] Zuazua, E., Propagation, observation, and control of waves approximated by finite difference methods, *SIAM Review* **47** (2005), 197–243.

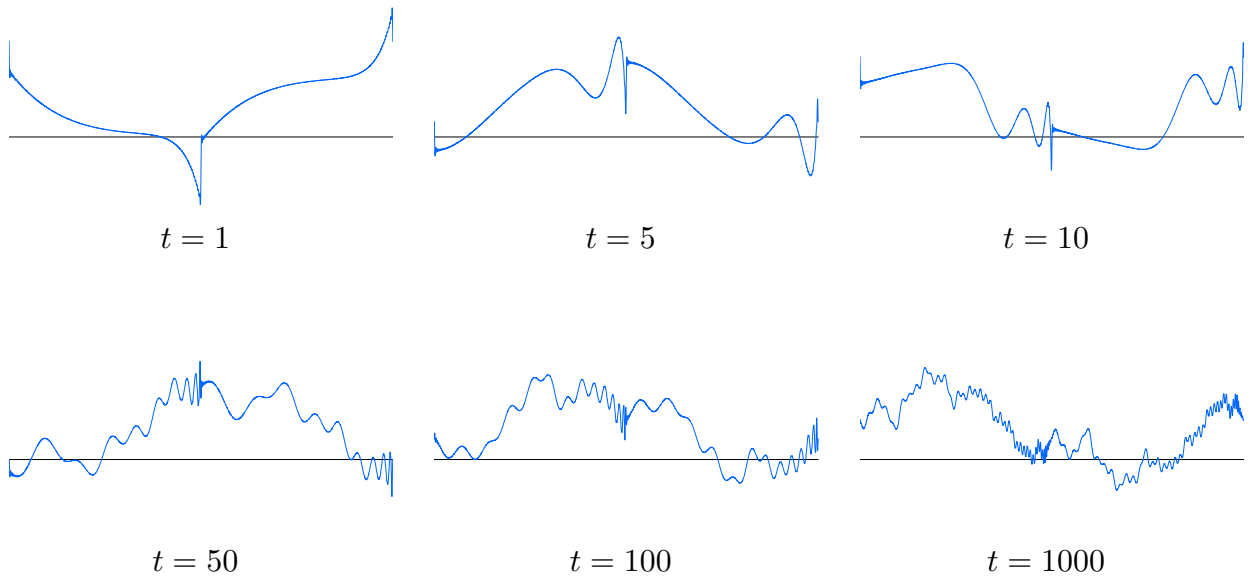


**Figure 2.** RLW/BBM Dispersion:  $\omega = \frac{k}{1 + \frac{1}{6}k^2}$ .

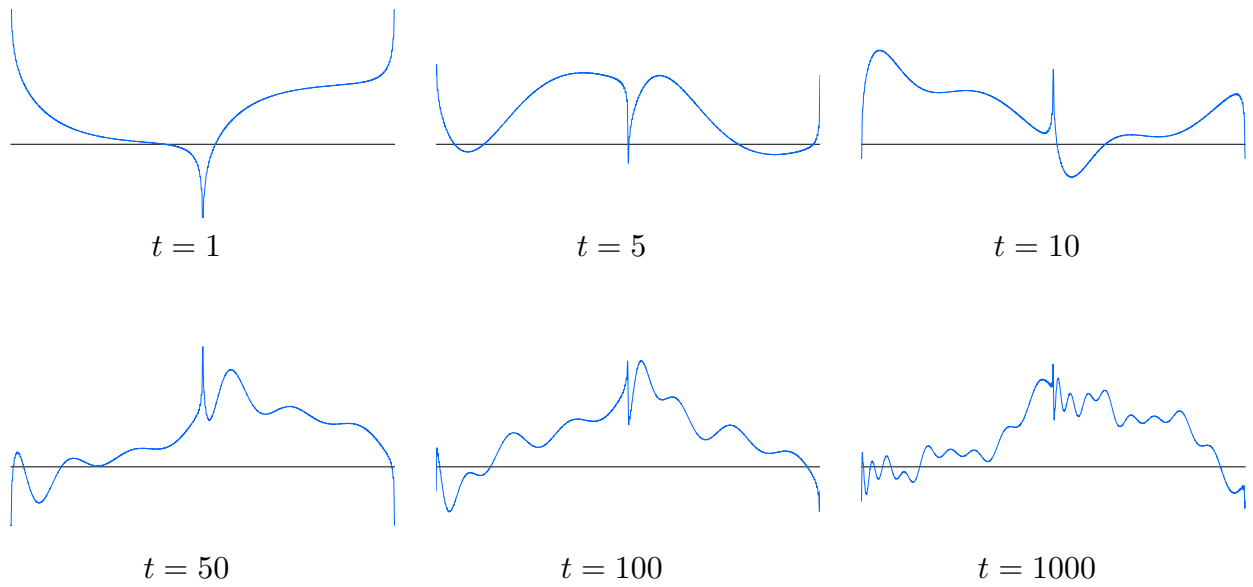


**Figure 3.** Regularized Boussinesq Dispersion:  $\omega = \frac{k}{\sqrt{1 + \frac{1}{3}k^2}}$ .

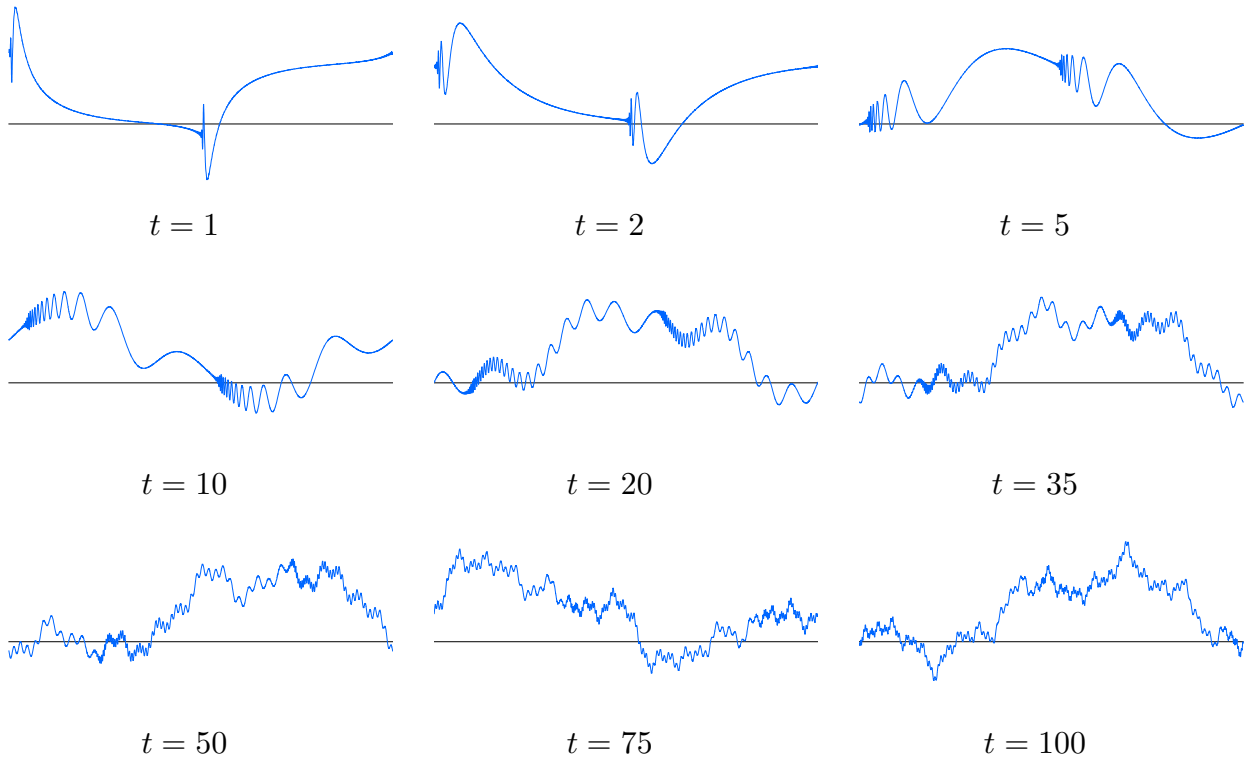


**Figure 4.** Water Wave Dispersion:  $\omega = \sqrt{k \tanh k} \operatorname{sign} k$ .

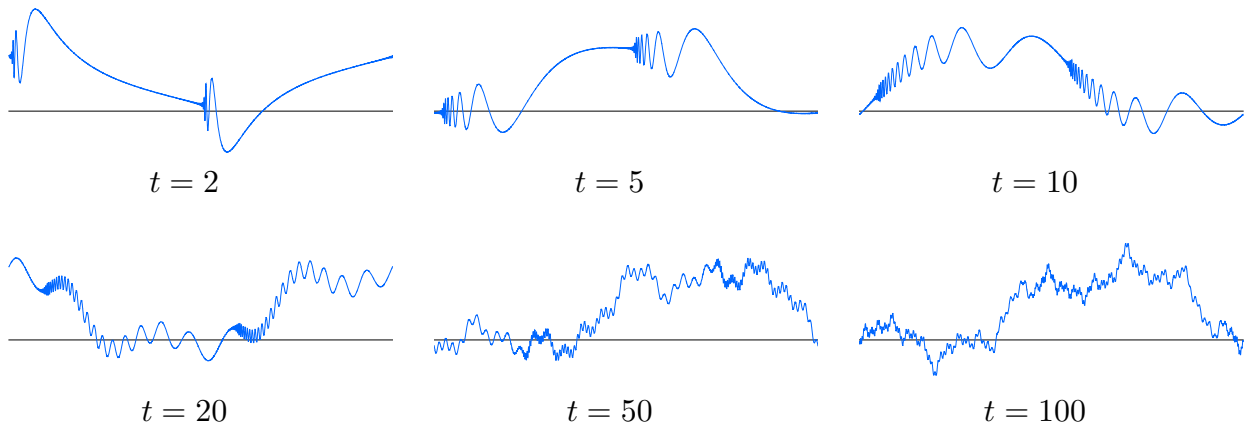


**Figure 5.** Square Root Dispersion:  $\omega = \sqrt{|k|} \operatorname{sign} k$ .

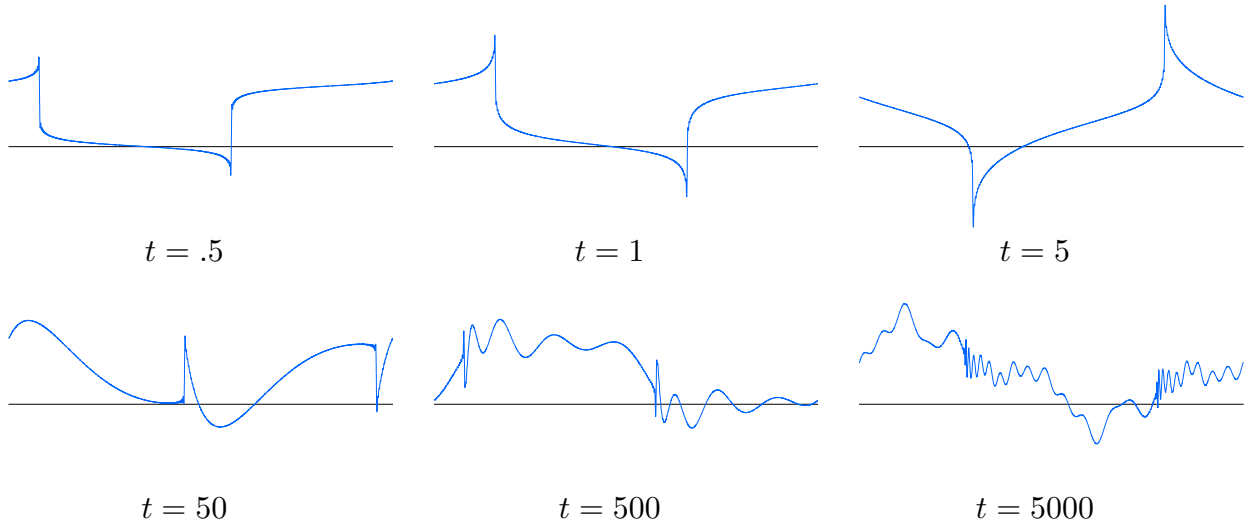


**Figure 6.** Asymptotically Linear Dispersion:  $\omega = \sqrt{|k(k+1)|} \text{ sign } k$ .

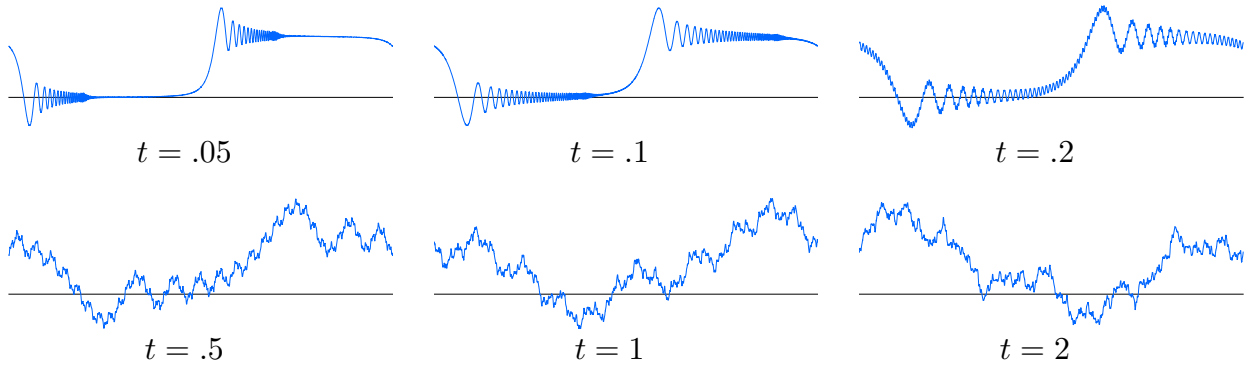


**Figure 7.** Three-halves Dispersion:  $\omega = |k|^{3/2} \text{ sign } k$ .

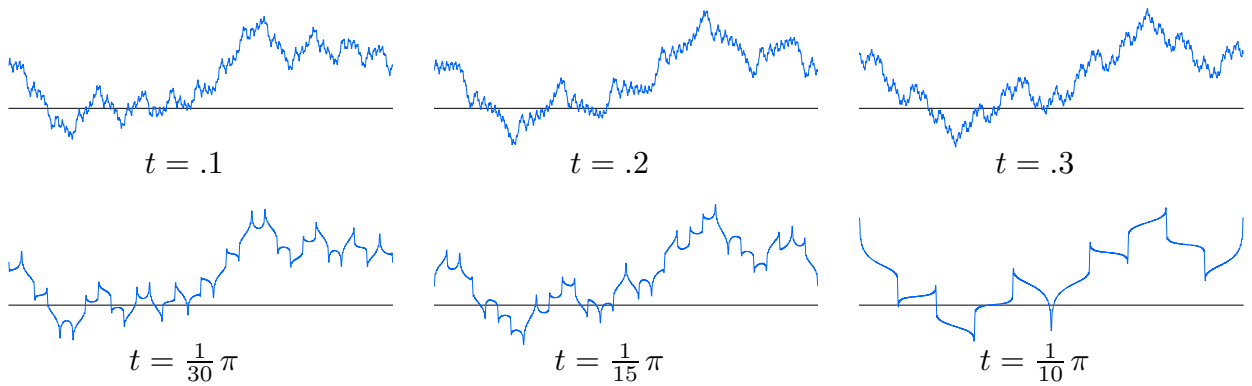


**Figure 8.** Benjamin-Ono Dispersion:  $\omega = |k|^2 \text{ sign } k$ .



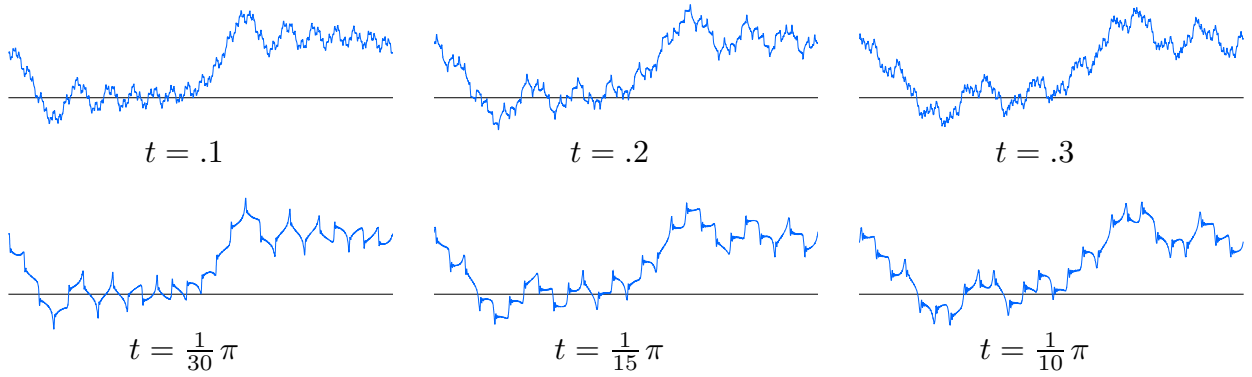


**Figure 9.** Integrable Boussinesq Dispersion:  $\omega = k \sqrt{1 + \frac{1}{3} k^2}$ .

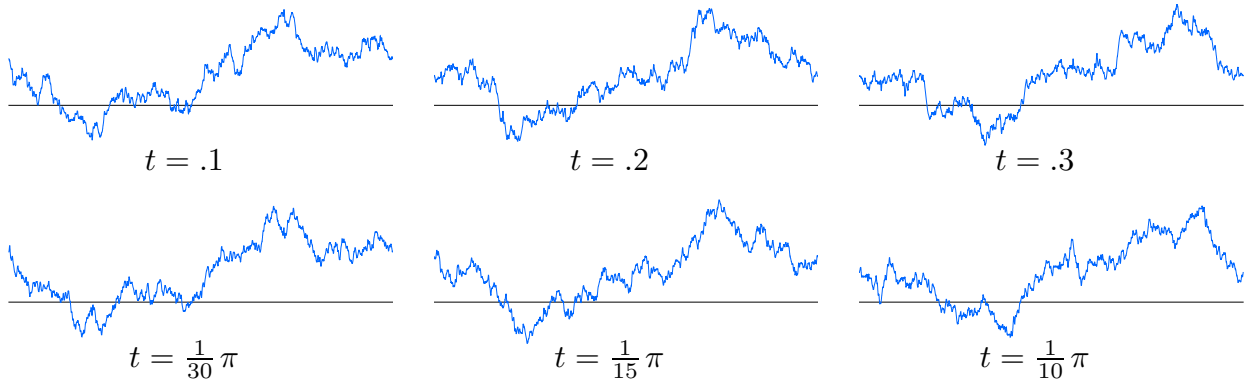


**Figure 10.** Five-halves Dispersion:  $\omega = |k|^{5/2} \text{sign } k$ .

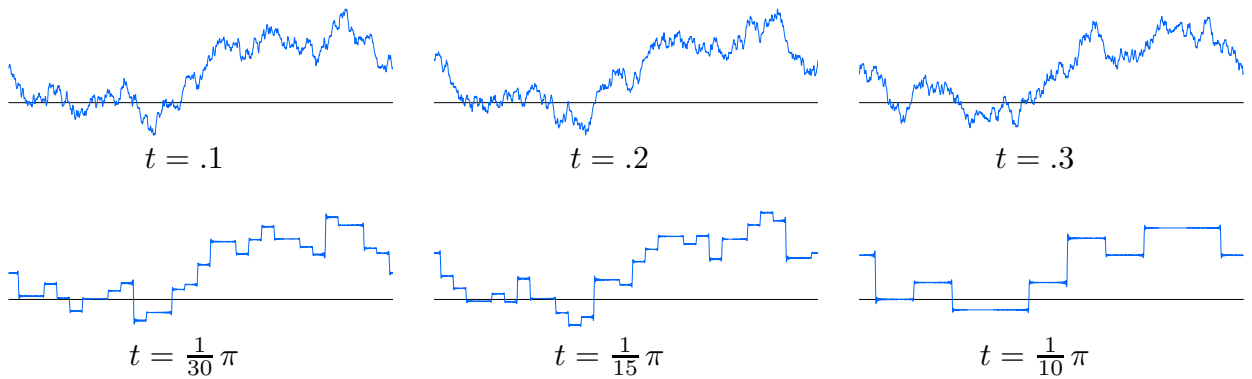


**Figure 11.** Korteweg–deVries Dispersion:  $\omega = k - \frac{1}{6} k^3$ .

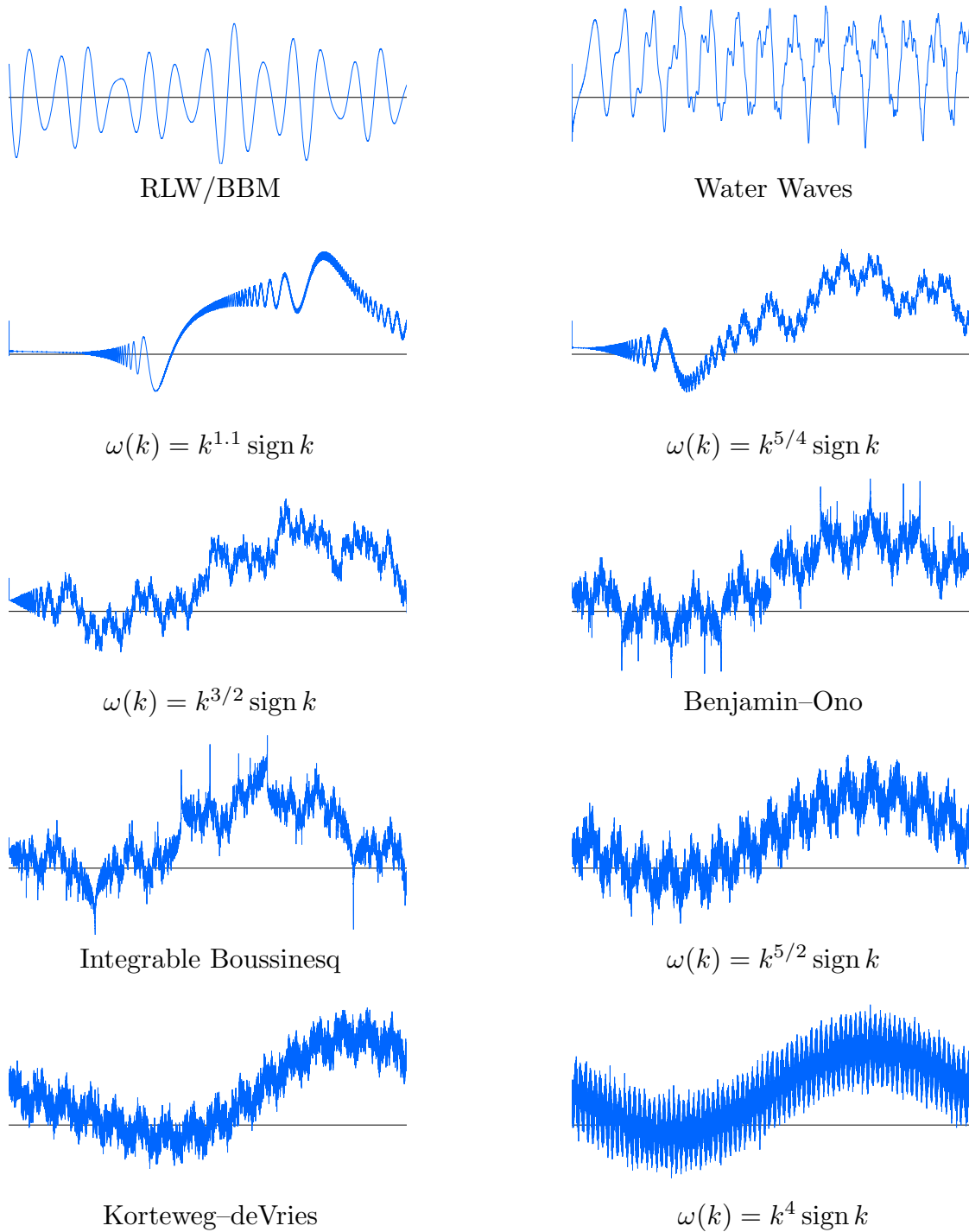


**Figure 12.** Plots of  $u(t, 0)$  for Representative Dispersion Relations.

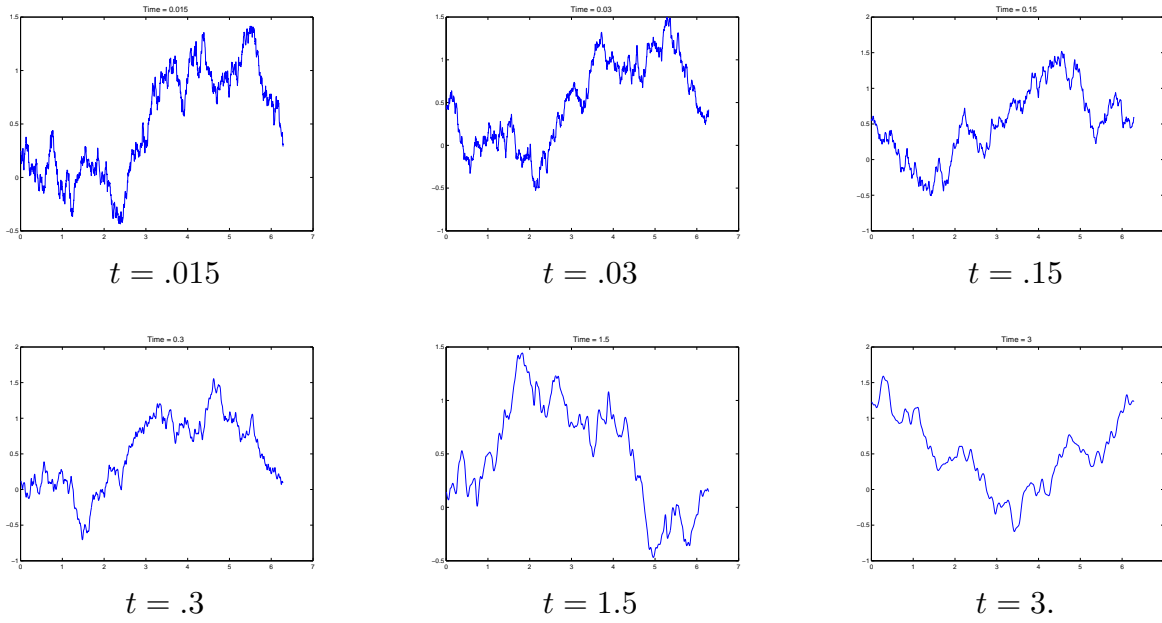


**Figure 13.** Korteweg–deVries Equation: Irrational Times.

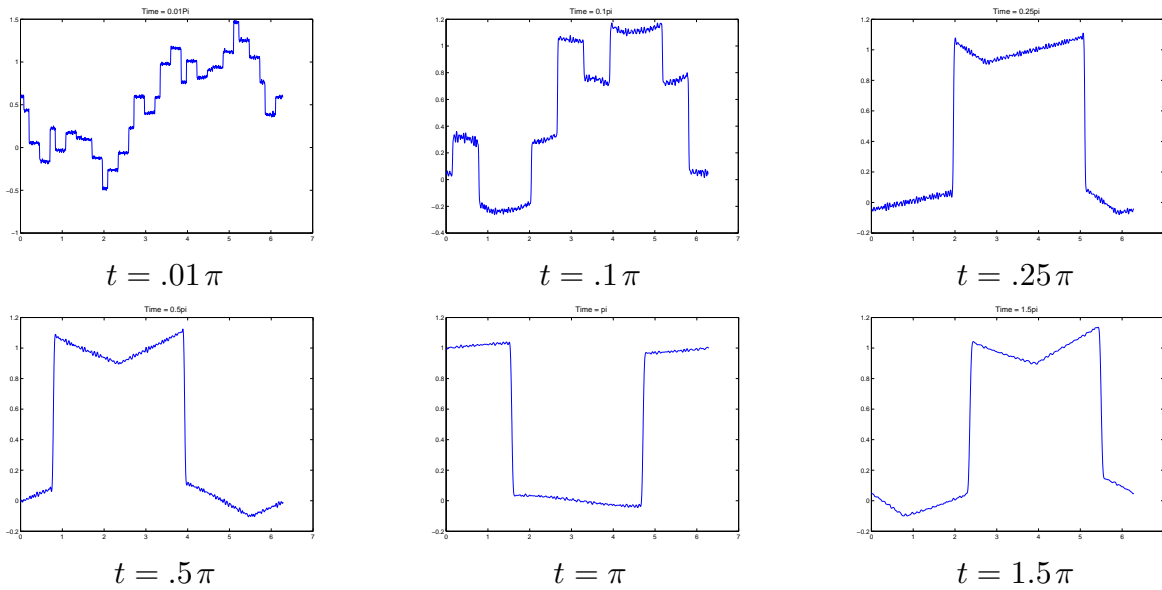


**Figure 14.** Korteweg–deVries Equation: Rational Times.

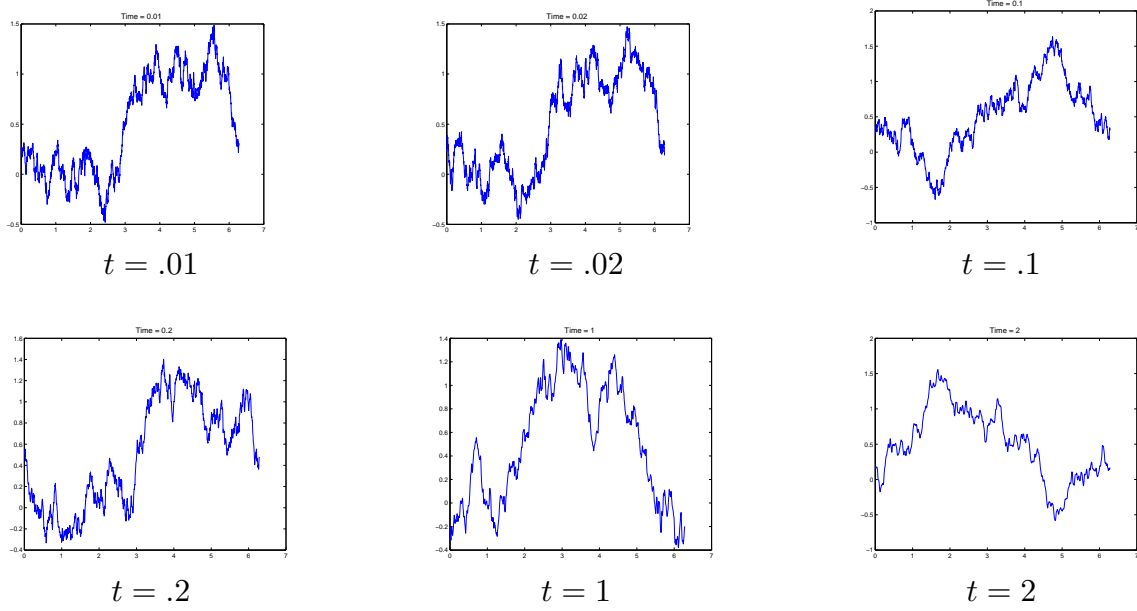


**Figure 15.** Quartic Korteweg-deVries Equation: Irrational Times.

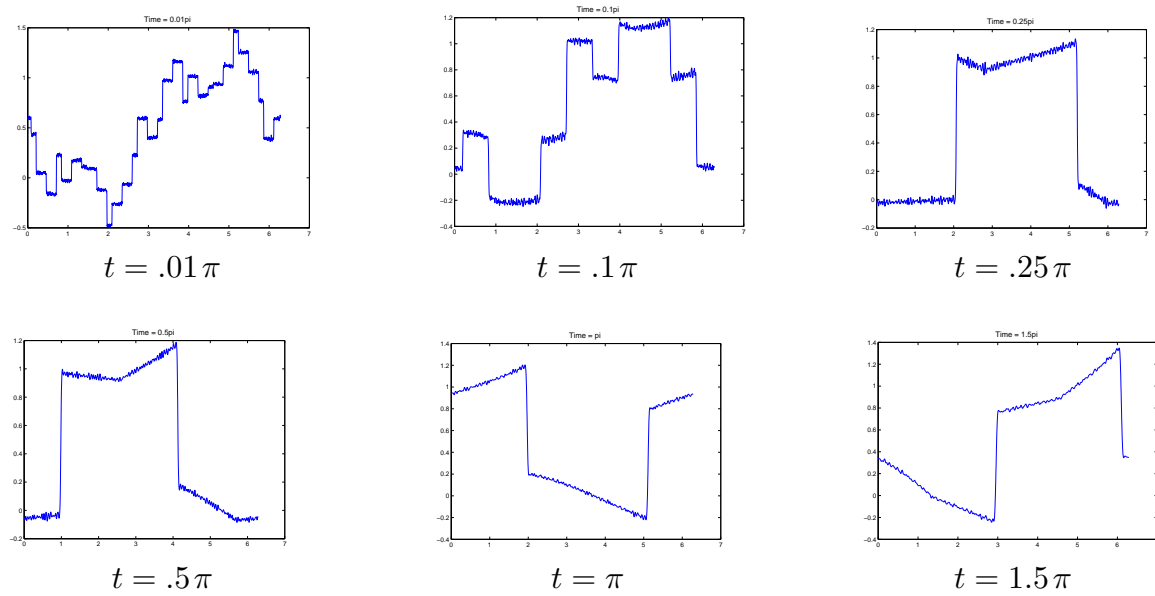


**Figure 16.** Quartic Korteweg-deVries Equation: Rational Times.